In Situ Characterization of Mobilization, Dispersion and Re-Settling in Impinging Jet Ballast Tanks with an Acoustic Backscatter System – 14097

Jaiyana Bux *, Timothy Hunter *, Neepa Paul *, Jonathan Dodds **, Dominic Rhodes **,
Jeff Peakall *, Simon Biggs *
* University of Leeds
** National Nuclear Laboratory

ABSTRACT

An ability to accurately characterize particulate suspensions is imperative in the nuclear industry. Particularly since there is an urgent need to retrieve legacy waste sludge and slurries, to enable post operational clean out (POCO) of aged and worn facilities. *In situ* measurements that remove the need for complex sampling protocols are especially preferred in this context. However, the large scale of many process unit operations on plant, with associated poor optical clarity, frequently make classical visual analysis routes for solids distribution impossible. Here, the application of an acoustic backscatter system (ABS) to enable the characterization of key features in solid-liquid systems is discussed. The ABS was deployed in a scaled non-active test rig mirroring Highly Active Storage Tanks (HASTs), which are buffer storage tanks for the penultimate liquor wastes generated from reprocessing at Sellafield. Specifically, sediment bed erosion by impinging jet ballasts, subsequent sludge re-suspension, solids dispersion via airlifts and sediment re-settling behavior were characterized, by taking ABS measurements in diverse jet operation cycles. The effectiveness of varying jet cycles and durations, neighboring jet influences, general sediment re-suspension and settling behavior, and the dispersive effectiveness of airlifts were ascertained and verified via independent sampling experiments. These findings translate to the HAST plant scenario, and thus enhance current operational knowledge and contribute to the modeling for POCO purposes. Ultimately the ABS's capability as a powerful *in situ* characterization tool in non-active liquid waste related applications is demonstrated.

INTRODUCTION

The management and disposal of wastes is a critical priority for the nuclear industry. In particular, there is a current need to retrieve legacy waste sludge and slurries, to enable post operational clean out (POCO) of aged and worn facilities. However, the complex and radioactive nature of the legacy sludge inventory, deems this task challenging. *In situ* measurements that remove the need for complex sampling protocols is especially preferred in this context, and would certainly benefit operations management and modeling for POCO purposes [1]. Although some *in situ* instrumentation exist on active plant, (e.g. turbidity meters and electrical impedance techniques), these are limited by one or more of the following caveats; operational in dilute suspensions only, suited to batch-scale experiments, complex and restrictive in terms of operational set-up or unable to provide solids depth profiles [2]. Acoustics, specifically the diagnostic ultrasonic range, can overcome some of these caveats to a practicable extent and enable flexible, non-intrusive, real-time measurement with high spatial and temporal resolution [1, 3, 4, 5]. For example acoustic waves can penetrate further than light waves [6], thus they offer the opportunity to characterize opaque and more concentrated suspensions. In particular the single transducer devices which generate and propagate high frequency pulses through suspensions and provide characterization with respect to the measured echo return, offer the

highest flexibility in terms of application as an entire distance profile can be measured from a single measurement position [7]. The measured backscattered intensity or the level of signal attenuation can elucidate variables such as particulate concentration, size, aggregation, flow velocity, and visualize sedimentation processes [8, 9, 10]. These features are especially beneficial for the characterization of numerous industrial suspensions. In fact, low frequency ultrasonic probes are currently utilized as monitors to determine the position of sludge blankets in clarifiers and thickeners [11, 12], however it is not currently possible to ascertain concentration or segregation information using these devices.

Currently, ultrasonic probe systems are extensively utilized for sediment transport studies in marine and freshwater environments [13, 14, 15], where solids concentrations are dilute, typically less than 0.1 g/L [8]. Recently Hunter et al. [10, 16] demonstrated the potential of extending the application of an acoustic backscatter system (ABS), to characterize more concentrated suspensions which more closely represent (although not fully), concentrations encountered in industry. For example spherical glass particle (~40 μm) suspensions of up to 10 wt.% solids were characterized across a 0.1 to 1 m depth range (depending on achievable acoustic penetration depth). Additionally, intricate hindered settling processes were monitored and concentration segregation owing to the segregation of size distributed particles was reported. Although the ABS technique has been previously reported to be limited to dilute applications under the traditional theoretical characterization approach [8], Hunter et al. [10] suggest an alternative phenomenological approach whereby the rate of backscatter signal attenuation is empirically correlated to concentration above an approximate 2.5 g/L threshold for glass particle suspensions. Moreover, the current authors applied this empirical technique and successfully characterized concentrated (0.5 – 10 wt.%) titanium dioxide particle (~2 μm) suspensions. Here, analogous intricate settling behavior was identified in an industrially important colloidal mineral dispersion. This device has also recently been demonstrated to characterize particle size where a multiple frequency approach is required [17].

In this paper, we investigate extending the empirical approach to characterize a nuclear test material suspension within a realistic industrial setting. Specifically a non-active $4/10^{th}$ scale rig (FTR) resembling a highly active storage tank (HAST) is characterized at the National Nuclear Laboratory. HASTs are essentially buffer storage tanks for the penultimate highly active liquor (HAL) wastes generated from spent nuclear fuel reprocessing prior to vitrification. The cyclic operation of components within the tanks; impinging jet ballasts, cooling coils and air lifts, keep heat generating radioactive particles in suspension and prevent the formation of radioactive hotspots from sedimented particles on the base of the tank. HASTs are complex systems and due to the radioactive nature of the stored liquor wastes, they are difficult to monitor. Currently temperature measurements are employed to gauge whether radioactive hotspots exist within the plant. This method of monitoring could be improved as it does not confirm whether the sediment has been eroded from the HAST base in its entirety. Furthermore, currently it is not possible to visualize the distribution of the suspension within the HASTs. This is problematic from an operational viewpoint when routinely storing and transporting radioactive suspensions, but it also presents significant monitoring and modeling challenges from a POCO perspective. Thus understanding suspension dynamics and the ability to monitor the system is imperative [18]. Specifically sediment clearance by jet erosion, sludge re-suspension dynamics and sediment re-settling behavior is of interest for the development of computational models [19], and is investigated here with a commercially available ABS.

DESCRIPTION
Materials

Barytes (barium sulfate supplied from RBH Ltd, UK) was utilized as the non-active nuclear test material suspension in water. HAL comprises numerous chemical species [18] but only the solids are really of interest in this experiment. Although on plant HAL exists in nitric acid suspension, scaling down to 40% in the FTR corresponds dynamically with a water suspension of similar viscosity. Generally non-radioactive experiments are conducted with either simulants which are non-active analogs, or test materials which are essentially natural minerals which exhibit some analogous properties to the active particles. Owing to the large experimental scale of the FTR, utilizing test materials is the cost effective option [18].

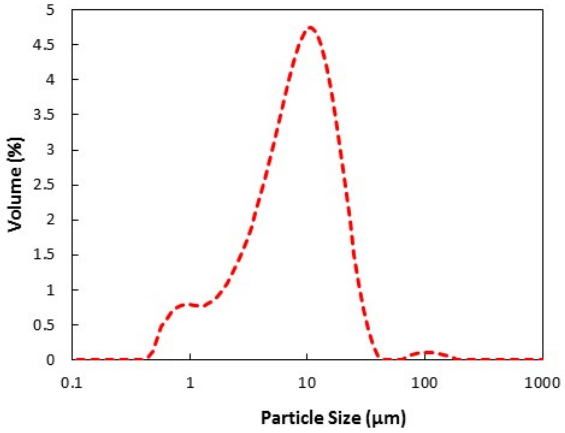

Fig.1. Barytes Particle Size Distribution

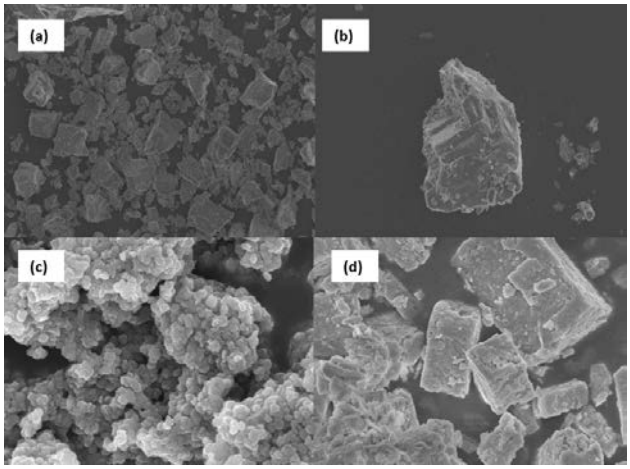

Fig.2. SEM images of Barytes at (a) x 2,5k and (b) x 10k magnification,(c)CPM analog [18] and (d) ZM analog [18]

Cesium phosphomolybdate (CPM) and Zirconium molybdate (ZM) are the two major solids components of HAL [18]. When selecting a test material, consideration must be made as to whether its physical properties resemble those of CPM and ZM to a practicable extent. Various test materials were considered for FTR experimentation however Barytes made an interesting case for numerous reasons. Essentially, modelling erosion, solids resuspension and settling are the key parameters of interest with respect to this particular rig. Hence material density, which invariably influences resuspension and settling behavior, is the critical parameter to consider. The density of Barytes was measured via a Micromeritics Accu-Pyc 1330 helium pycnometer (Micromeritics Instrument Corporation, USA), the average value of which was determined to be 4.42 g/cm^3. The densities of CPM and ZM are established to be in the region of 3.4 – 4.0 g/cm^3 [18, 20]. Comparatively the density of Barytes is greater than that of the HAL constituents and thus could potentially provide a worst case test material scenario in terms of settling, whereby the denser Barytes would potentially settle more rapidly than the HAL constituents. Also its settling properties are thought to correlate with the 40% scaling of the rig [23]. Additionally particle size and shape also influence settling and sediment bed packing. The particle size distribution of barytes obtained via a Malvern Mastersizer 2000 (Malvern Instruments Ltd, UK) is presented in Fig.1. The distribution is close to bimodal with a D_{50} of 7.8 µm and a significant fraction of fines. Given that the typical D_{50} of ZM is 9 µm [20], barytes may in fact be a close analog of ZM with respect to particle size. CPM is relatively smaller with a D_{50} of 0.9 µm.

Furthermore SEM images of barytes obtained via a FEGSEM (University of Leeds, UK) are presented in Fig.2. for (a) x 2,500 and (b) x 10,000 magnification, alongside those obtained by Paul et al. [18] for (c) CPM analogue simulant and (d) ZM analogue simulant. Upon comparison, Barytes exhibits an irregular crystal structure, and although ZM exhibits a specific cuboidal structure, the two can be assumed to exhibit a closer shape profile match when compared with CPM which has a spheroidal structure of aggregated particles. Furthermore, Barytes is cohesive thus potentially provides a sediment bed which could be challenging to resuspend if left to compact for extended durations, thus providing a worst case test scenario with respect to erosion and resuspension. Notably there numerous other considerations to be factored when conducting experiments on such a large scale. For example, Barytes is a relatively safe (i.e. non heavy metal based) material and can be used in large quantities of water which eases disposal. It is also a relatively cheap material and can be acquired in large quantities with ease.

FTR – ABS Experimental Set-Up

The FTR is a 40% scaled down version of a HAST. The system comprises of 'mock' jet ballasts which essentially withdraw fluid from the tank (rather than use steam ejectors) and fires it out at a known velocity, creating an impingement which erodes and resuspends the sediment bed from the tank base [21]. Several jet ballasts which are operated in sequence, with numerous cycles performed daily on plant. In addition, cooling coils occupy a significant volume of the HASTs, removing heat generated from radioactive HAL; 'dummy' coils are located in the FTR to replicate this for obstruction. Air lifts are another major component of the tanks and are situated in the near base region of the HAST creating a homogenous suspension. They operate by injecting air into the suspension liquor and serve to further disperse suspended particles throughout the HAST. They are usually only operated prior to HAST decantation. In Fig.3(a) a schematic of the FTR is presented whereby the positions of the six peripheral jet ballasts, the central jet ballast, the four airlifts and the location of the ABS during experimentation are shown. Detailed experimental positioning of the ABS is illustrated in Fig.3(b). The ABS utilized here is an AQUAscat 1000 (Aquatec Group Ltd, UK) equipped with a 1 MHz and 2 x 2 MHz transducers which were simultaneously deployed.

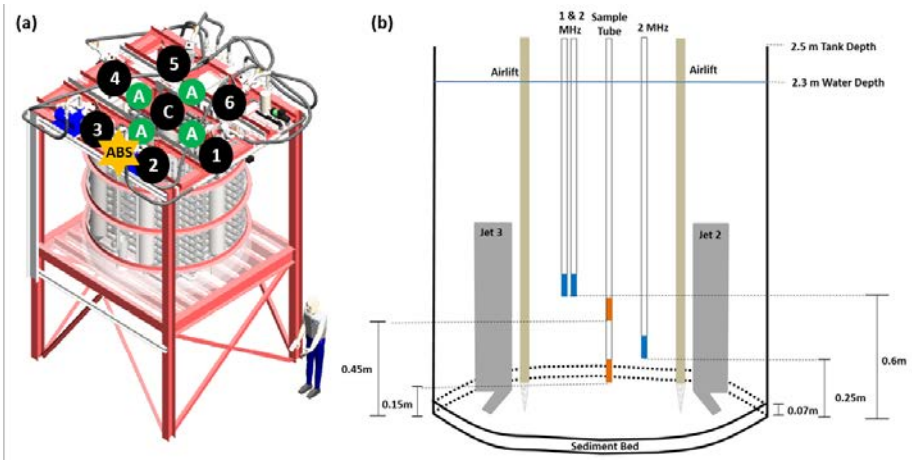

Fig.3. (a) FTR schematic denoting positions of one central and six peripheral jet ballasts, four airlifts and the ABS position during experimentation and (b) ABS and sampling port positions

The region between Jet 2 and Jet 3 provided the only access point into the FTR at the time due to the many components within the tank. This resulted in a very narrow detection region, free from significant cooling coil interference. For ABS, a lower probe frequency leads to a reduced signal attenuation and a greater depth penetration [10]. Hence, here we use the 1 MHz transducer positioned approximately 60-80 cm from the base to monitor large length-scale suspension changes. However, lower frequency probes also have a lower resolution and are less sensitive to subtle changes in suspension concentration with distance [10]. Hence, in the near bed region, where the bulk of solids is expected to reside [22], a 2 MHz transducer was positioned at approximately 25-30 cm from the base. Additionally, a second 2 MHz transducer was situated adjacent to the 1 MHz probe in the upper region to enable additional higher resolution characterization in approximately 30 cm of the upper profiling region. A transducer pulse repetition rate of 64 Hz was operated with one full depth profile collected every second. The depth profiles were segregated into 5 mm measurement bins.

Several jet ballast operating regimes were employed to investigate variously; the efficiency of erosion, the influences of neighboring jets, different jet firing durations, the effect of cycle patterns, and tank internals on resuspension and subsequent resettling behavior. In addition, the effectiveness of airlifts was also investigated. The various regimes explored in this work are summarized in TABLE I. Regime 1 and 2 are analogous to those employed by Hunter et al. [22] in previous FTR experiments where the ABS was utilized to characterize erosion, resuspension and dispersion behavior in the presence of jet ballasts alone. Regimes 3 and 4 are more representative to those employed in actual HAST operation. Notably there are operational constraints (scaling, rig operation etc.) involved in large scale experimental rigs of this sort, which directly impacted regime selection. Furthermore 60 minute inoperative periods were allowed to elapse between regimes, to provide a practicable time frame for sediment to resettle close to background levels. ABS measurement commenced upon firing of the final jet (anticipated maximum solids suspended) in each regime and ceased by 30 minutes post firing. It was previously established that the sediment resettled close to background levels well within a 30 minute time frame [22]. Moreover one minute background readings were taken in between regimes.

TABLE I. FTR Experimental Regimes

Regime	Jet Sequence	Jet Burst	Fill	Airlifts	Sampling
R1	Jet 1	40 mins	50%	-	-
R2	Jet 1 + Central Jet	40 mins	50%	-	-
R3.1/2/3	2 x clockwise cycles with 100s delay between jets; Jet 5+C, 6, 1, 2, 3, 4	20 sec	50%	-	-
R4	2 x clockwise cycles with no jet delay; Jet 4, 5, 6, 1, 2, 3, Central Jet continuous	20 sec	100%	1 x run with continuous operation 1 x run without	2 x experimental depths extracting 2 x 20 ml at 0.5-2 min intervals

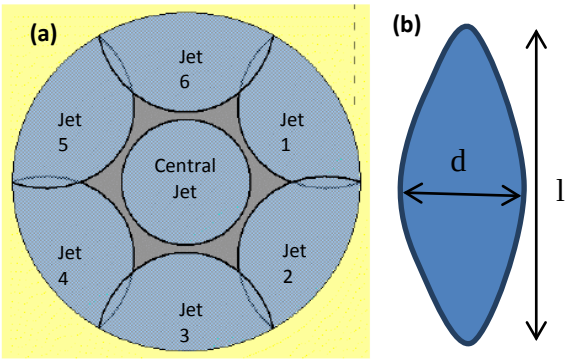

Fig.4. (a) Sediment clearance model via impinging jet ballasts and (b) measurements taken [21]

Since the FTR is supported on a platform, it was also possible to access the underside of the tank to directly measure sediment clearance of each jet. A representation of the expected jet clearance pattern is presented in Fig.4 (a). The peripheral jets form an erosion profile akin to the image in Fig.4 (b) for which the length and diameter were measured. The diameter of the circular Central Jet profile was also measured. Finally it was also possible to conduct independent sampling experiments post ABS measurements during Regime 4, in order to gauge physical solids concentration changes to compare with the ABS data. Accordingly sampling was initiated post firing of Jet 2 in the second cycle, and 2 x 20 ml samples were extracted with a peristaltic pump every 30 s – 60 s. An initial experiment extracted samples at 15 cm from the base (near-bed region), and the procedure was repeated in a second sampling experiment to extract samples at 45 cm from the base, (refer to Fig. 3(b) for locations).

DISCUSSION

Regimes 1 - 3; Erosion, Resuspension, Dispersion and Resettling

Testing Regimes 1 – 3 were used to compare the effectiveness of various jet cycles and durations on solids erosion, resuspension, dispersion and resettling. In addition, the effects of neighboring jet influences were also explored. The backscatter response from the ABS for the Barytes suspension immediately following each firing regime is presented in Fig. 5. These data represent suspension conditions at T_0, referring to the ensemble average of the first five seconds/profiles of measurement, (data were collected at one complete tank depth profile per second). In addition, Regime 3 is split into three separate components corresponding to measurement directly after the firing of Jet 2 (R3.1), Jet 3 (R3.2) and Jet 4 (R3.3) during the second cycle.

Fig. 5 provides data that are typical of backscatter intensity with respect to position from the transducer head whereby the strongest signal is received closest to the transducer head and the intensity is naturally attenuated with increasing distance away. Note the signal analysis cut-off point is arbitrarily set here at -70 dB and therefore data below this level should be discounted. Another typical yet important observation is the narrow peaks to the right of Fig. 5 (a) & (b). Regions that are relatively dense, for example a supernatant-sludge interface or hard tank walls, behave as strong scattering planes. When referring to the peak locations in Fig. 5, it is supposed that these correspond here to a sediment bed on the base of the FTR. This inference is supported by the observed peak shifting to the right by a few centimeters, away

from the transducer position, in Regime 3. The higher resolution 2 MHz transducer positioned in the near-bed region between Jet 2 and Jet 3 (Fig. 5 (b)), depicts a 1 cm bed depth reduction at R3.1 (post Jet 2), a total reduction of 2 cm at R3.2 (post Jet 3) and erosion depth remains stagnant at minus 2 cm at R3.3 (post Jet 4 – furthest jet from ABS of the three measured). Furthermore, the position and depth of the bed in the ABS measurement location (between Jet 2 and Jet 3) remains unperturbed post Regime 1 (corresponding to firing of Jet 1) and Regime 2 (corresponding to firing of Jet 1 and Central Jet). These observations indicate that sediment bed erosion via the jets is localized and that the jets do not influence erosion in neighboring jet regions. The influence of neighboring jets is a matter of concern from an operational point of view. For example, it would be problematic if the HAL sediment simply sweeps from the base of one jet location to the base of another upon firing, rather than resuspending. It is evident here, however, that the jets do not erode sediment in neighboring regions or sweep sediment across the base.

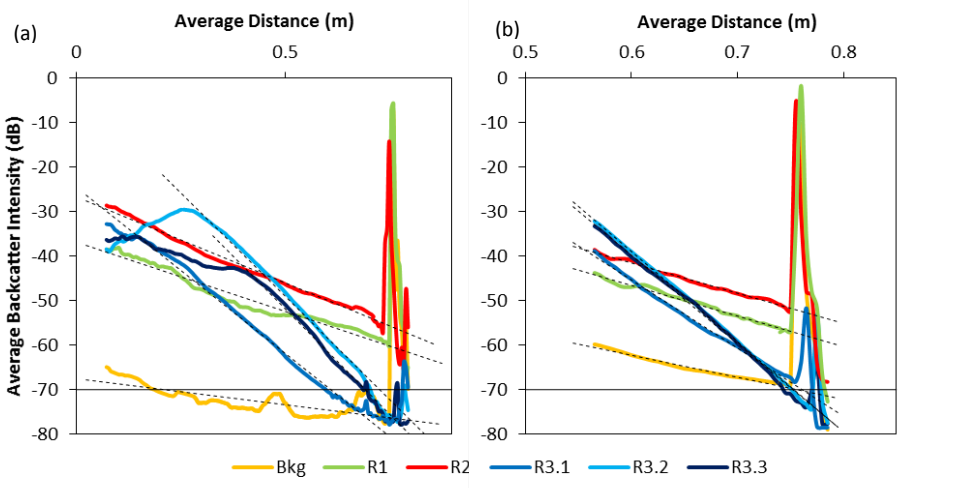

Fig. 5. Time averaged backscatter response at T_0 during settling with respect to the mean distance from transducer; (a) 1 MHz (75 cm from base – entire profiling region) and (b) 2 MHz (25 cm from base – lower profiling region), where ___ at -70 dB represents the signal analysis cut-off point and - - - represents linear attenuation rates

The observations from this work do not confirm whether the bed was eroded in its entirety within the measurement location. Referring back to the model of expected jet clearance in Fig.4, the blue regions depict expected sediment clearance by the corresponding jet and the grey shading depicts a dormant bed region where erosion doesn't occur. Such a region is of concern with respect to radioactive hotspot formation, however the only method from plant to indicate the presence of such an area is limited thermocouple data. Interestingly from visual observation of the FTR sidewall prior to experimentation, a bed depth range of 5 – 7 cm was observed around the circumference of the FTR, inferring bed inhomogeneity. Immediately preceding each regime, no erosion was witnessed at the side-walls. Additionally upon observation beneath the base, uniform clearance patterns were not formed and the entire bed was not eroded from the base at any point in time. This is perhaps the result of utilizing a dense and cohesive test material (Barytes). Evidently Barytes erosion doesn't follow the expected clearance model and presents a problematic scenario if the HAL suspension were to behave in an identical manner in a general operation or POCO scenario.

Moreover the peaks for R3 are markedly weaker than that of R1-2, which is expected since no erosion had occurred in the measurement region for the former two regimes. However interestingly, R3.3 in Fig. 5(b) portrays greater reduction in peak intensity than R3.1-2. The former represents conditions at the end of the jet firing cycles, by which point the maximum possible sediment resuspension has been achieved. Consequently it is likely that a higher solids concentration has been achieved in suspension by R3.3, thus is attenuating the peak backscatter intensity to a greater extent.

Secondary broad peaks are detected at 50 cm above the bed at R3.2, and 40 cm above the bed at R3.3, by the 1 MHz transducer profiling the largest distance from the base (see Fig.5 (a)). R3.2 represents the point in time directly after the successive firing of Jet 2 and Jet 3 in the second cycle, by which point a relatively significant concentration of particles will have accumulated in suspension. It is hypothesized that this resuspension and subsequent settling of a significant particle concentration will result in a sludge-supernatant interface. The broad peak at 50 cm corresponds to this interface. In previous work, Hunter et al. [22] identified that although the jets are good at resuspending sediment, they are poor at dispersion and homogenization, resulting in a fluidized bed within the base region. The presence of a sludge-supernatant interface at approximately 50 cm from the base of the tank is consistent with this hypothesis. Subsequently by time R3.3, the broad peak has receded to approximately 40 cm from the bed. The reduced sludge-supernatant interface height here corresponds with measurement taken directly after the furthest jet (of the three measured), where reduced neighboring jet influence is known. Since Barytes is dense and known to be rapid settling in the FTR context [22, 23], the drop in height is consistent with a settling suspension. The settling rate between R3.2 and R3.3 approximates to 0.8 mm/s, analogous to that observed by Hunter et al. [22]. These observations highlight the ABS's capability as a sludge resuspension monitor.

In addition, further valuable information can be extracted from the data shown in Fig. 5. Typically an ABS is utilized as a concentration monitor since backscatter intensity and attenuation directly correlate with solids concentration in suspension, where increasing concentration attenuates the backscatter intensity via absorption and augmented non-directional scattering. Concentration can be directly calculated from intensity data in dilute regimes if the particle backscatter and attenuation coefficients are known. These are not established for irregularly shaped Barytes particles and instead the phenomenological approach of Hunter et al. [10] can be taken, whereby an empirical relationship is established between relative changes in backscatter intensity or attenuation as a function of solids concentration. The average signal attenuation (dB/m) experienced in each regime was estimated assuming a linear drop in signal strength with distance (on the given dB scale) with the slope equating to the overall average drop for each time profile. These decay slopes are shown by the dashed lines in Fig. 5. From brief inspection it is evident that each regime displays a different backscatter decay slope, denoting variations in signal attenuation which indicates differences in suspended sediment concentration between these regimes. The average attenuation per regime is shown in Fig.6 for both frequency probes.

It is immediately evident from Fig. 6 that the 2 MHz probe experiences increased signal attenuation by comparison to the 1 MHz. The frequency – attenuation relationship is directly proportional [6] and so this observation was anticipated. It is also notable that both sets of data follow a similar trend with R3.1-3.3 exhibiting greater attenuation than R1-2, inferring higher concentrations of resuspended particles in the former, which is in agreement with the sediment bed erosion discussion. Hence, we can see that regime 3 is more successful at sediment

resuspension in the measurement zone whilst Jet 1 and the Central Jet, which are further away, generate poor resuspension in the ABS profiling location. This suggests that resuspension is significantly hindered by the presence of the cooling coils in this study. Hence it is likely that any sediment resuspension will be heterogeneous and localized around jet positions. Unfortunately, attenuation changes could not be verified or correlated with direct concentration values here due to the absence of physical samples in this test case. Nonetheless, the ABS data successfully demonstrated the powerful capability of this approach as a concentration and operational process monitor.

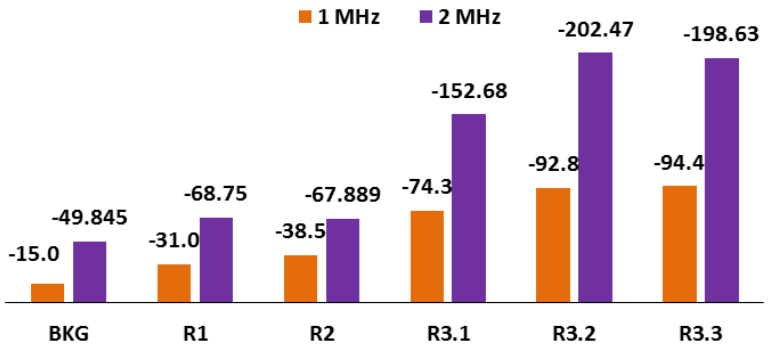

Fig.6. Backscatter attenuation (dB/m) at 1 MHz and 2 MHz for each regime

One other consideration which is important from an operational viewpoint, is the success of varying regimes with respect to jet firing durations [21]. According to the lack of erosion and resuspension activity of R1-2, it appears that the prolonged firing durations of R1-2 were the least successful at resuspension. Thus implying that lengthy jet bursts may be unnecessary and inappropriate in HAST operation. However this postulation wasn't substantiated in a like for like comparison and would require further investigation. Collectively, the observations thus far highlight the ABS capability in monitoring sediment bed erosion, dispersive success, settling rates and ultimately enable comparison of operational processes. It has been demonstrated in this context that the ABS is a powerful tool for *in situ* process monitoring.

Regime 4; Airlift Dispersion

The primary function of airlifts in the HASTs is to disperse and homogenize sediment throughout the tank post jet erosion. To gauge their dispersive effectiveness, Regime 4 was employed, firstly without airlifts and subsequently with airlifts in constant operation during jet ballast firing. Moreover, these experiments were conducted with ABS measurement, and later repeated as sampling experiments. The sampling experimental results are depicted here in Fig. 7 which gives the average solids concentration obtained at two heights; 15 cm (green) and 45 cm (red) above the base. All four sampling experiments show a decreasing trend for the solids concentration in suspension, from 2 minutes post jet ballast cycle completion consistent with sedimentation, as expected. Comparison of the concentration with and without operational airlifts, shows that the concentration is markedly lower for the former. This result infers the dispersive success of the airlifts, i.e. the reduced solids concentration denotes better solids dispersion away from the localized sampling position within the FTR tank. Furthermore, although homogeneity wasn't tested via lateral sampling position changes within the tank, an improved level of homogeneity is still inferred by the diminished concentration fluctuation exhibited with operational airlifts.

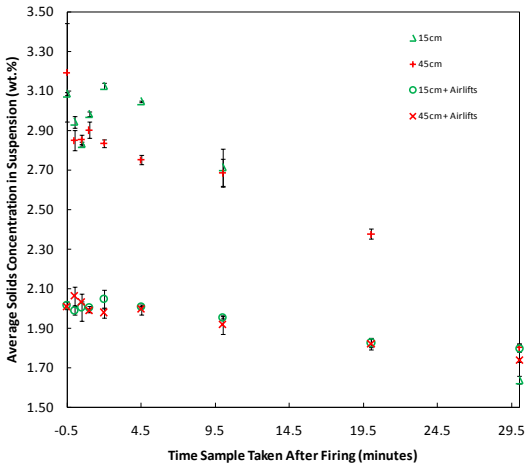

Fig.7. Solids concentration with respect to time at two heights, with and without operational airlifts

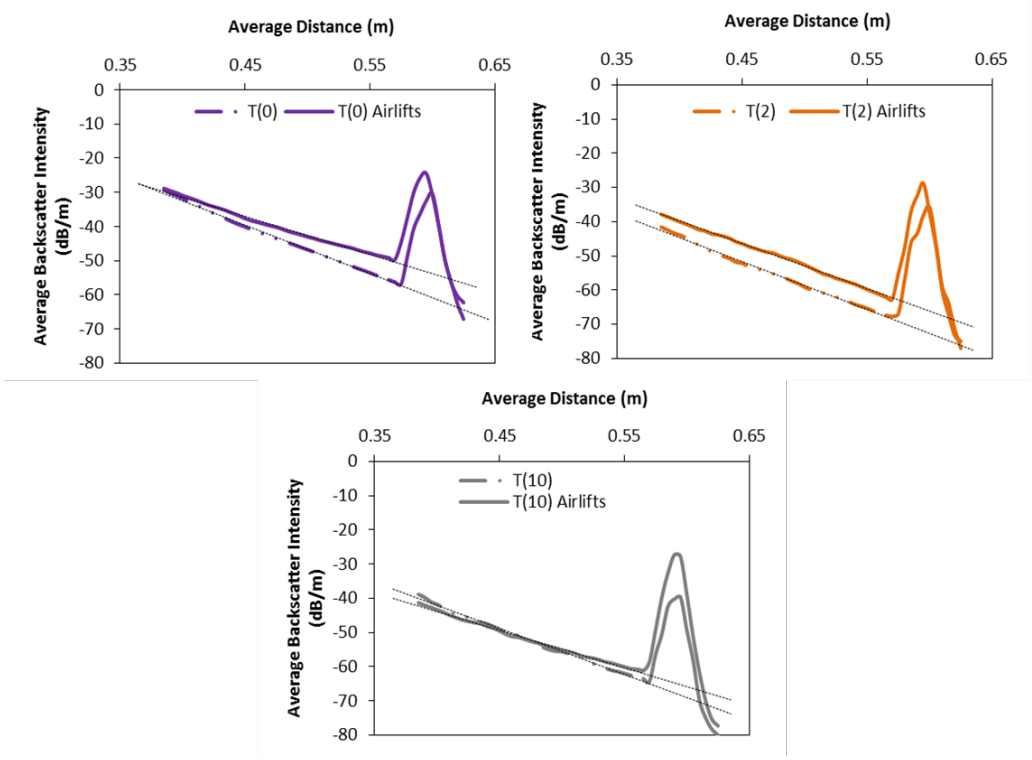

Fig.8. Average backscatter intensity of the 2 MHz transducer positioned in the lower region with and without operational airlifts at 0, 2 and 10 minutes post jet cycle, where - - - represents linear signal attenuation

Fig. 8 shows an example of the average backscatter intensity profiles obtained in analogous ABS experiments with and without operational airlifts. Data for the 2 MHz transducer in the near-bed region of the tank are given here with the response at T_0, T_2 and T_{10} minutes post jet-cycle being shown. These backscatter profiles are consistent with those previously presented, whereby there is a linear decay in backscatter intensity with increasing transducer range, and a prominent peak indicating that the sediment bed position is visible. At T_0, i.e. directly after firing

cycle cessation, the gradient of signal attenuation is steeper without operational airlifts inferring that the concentration is higher here and the jets alone are less successful at particle dispersion beyond the localized region within the tank. By T_2, the attenuation of the two scenarios is identical indicating similar concentration, although there is a discrepancy with respect to backscatter intensity. Barytes concentration – attenuation calibrations would need to be conducted in separate laboratory experiments before a definitive conclusion can be made. Finally by T_{10}, both scenarios depict analogous backscatter intensity and similar attenuation, although once again that without operational airlifts is slightly higher, inferring higher localized concentration.

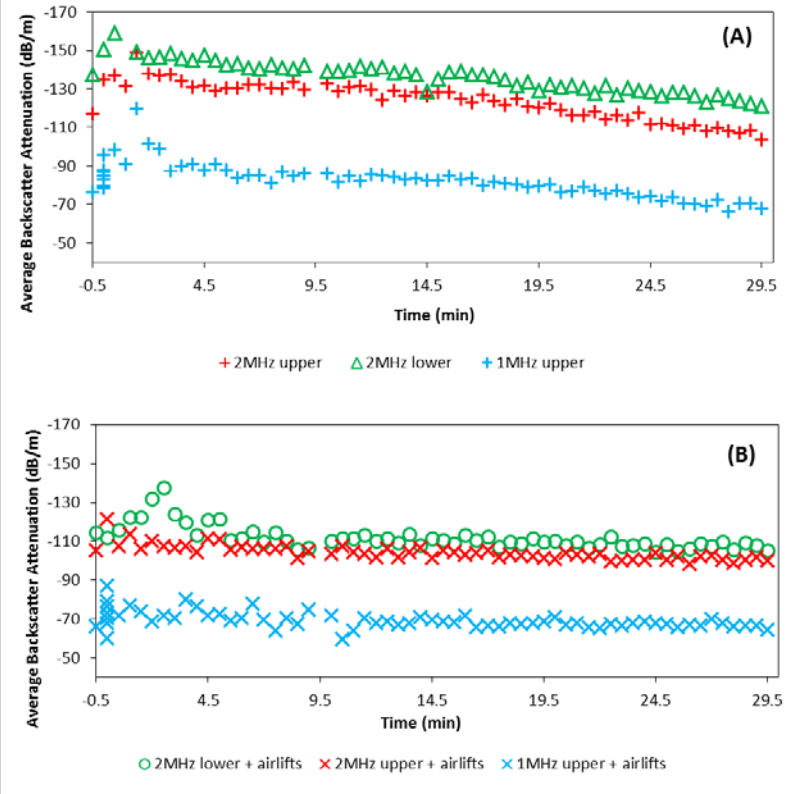

Fig.9. Average backscatter attenuation variations with time for (a) jet-only and (b) jet + continuously operational airlifts

The backscatter profiles for each transducer were then analyzed in more detail. The relative variations in linear attenuation (--- lines of Fig. 8) are given with respect to time in Fig. 9, where (a) and (b) correspond with jet-only and jet + airlift operation. From direct comparison of the two, it is evident that the attenuation values with operational airlifts are lower than those for the jet-only, inferring lower concentrations in the former. This concurs with the sampling experiments, where enhanced sediment dispersion is established with operational airlifts. Moreover both the ABS and sampling results depict a logical decrease in concentration from two minutes onwards, likely inferring sedimentation. It is also interesting to note that with operational airlifts (Fig.9 (b)), the level of attenuation is similar in both the upper and lower 2 MHz measurements indicating that depth-wise, the suspension is fairly homogenous.

Samples were extracted during independent Regime 4 sampling experiments to enable suspension particle size characterization via the Malvern Mastersizer 1000 (a laser diffraction

method for analyzing particle size). The particle size distributions obtained with and without operational airlifts at T_{30}, are presented in Fig. 10 (a). The distributions indicate that even after a 30 minute resettling period, there is a slight reduction in the particle size distribution of the jet ballast operation only, indicating some small percentage of coarse aggregates may have settled. However, this reduction is only relatively minor, suggesting the suspension retains a significant proportion of the larger Barytes particles when airlifts have been in operation during jet fire, thus inferring their dispersive effectiveness.

The particle size distributions of Barytes samples extracted at various stages are presented in Fig. 10 (b), whereby the D_{50} size is highlighted within the D_{10} to D_{90} percentile range. Firstly the size distribution with operational airlifts is depicted at three times; 0, 4.5 and 30 minutes after resuspension. Logically we see here that the particle sizes in suspension are reducing on a gradual time scale, which infers a gradual clarification of the liquor. Furthermore upon comparison of the two distributions at T_{30}, it is apparent that the D_{50} size and the size distribution of the suspended particles with jet-only operation is reduced more significantly with respect to the values when the airlifts are in operation. This correlates well to the previous observations that 'jet-only' operation achieves poor particle dispersion, and thus the clarification of fines proceeding initial bulk settling occurs on a more rapid timescale. These observations are key from an operational context, as they demonstrate the advantageous dispersion capability of airlifts within the HASTs.

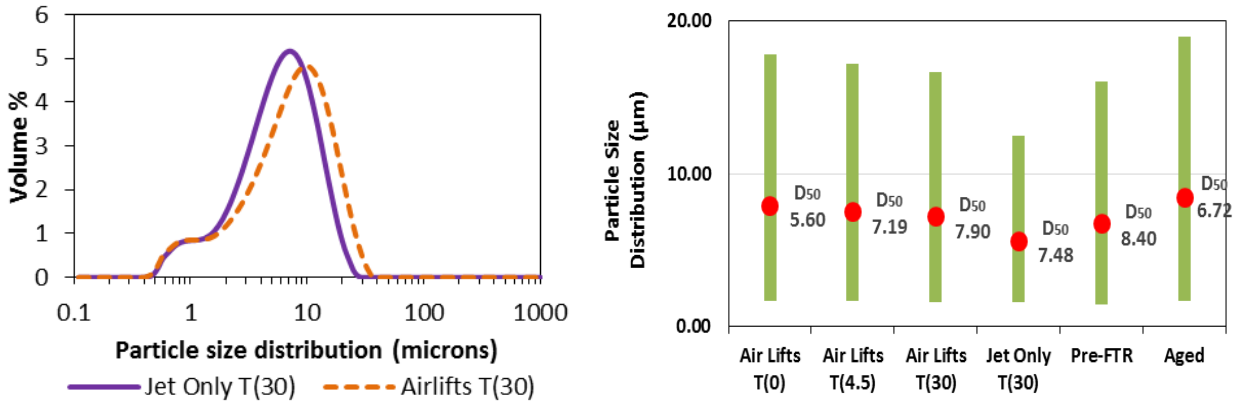

Fig.10. (a) Particle size distribution of barytes samples at T_{30} for jet-only and jet + airlifts, (b) size distributions of Barytes samples, where the D_{50} size is labelled within the D_{10} - D_{90} percentile range

Particle size distributions were characterized for the Barytes particles as supplied, prior to experimentation (Pre FTR), and that of the FTR's sediment bed (Aged). Here the Pre FTR percentile sizes are found to be larger than the jet-only sizes, demonstrating that the jets are in fact shearing the particles. This has implications in the real HAST scenario where radioactive particles are likely to be experiencing shearing on the real plant. Furthermore, the larger (aged) sediment bed sizes elucidate the cohesive nature of the Barytes. Should the bed remain unperturbed for lengthy durations, a cohesive sediment bed could prove difficult to erode. This has already been shown to be the case for the Barytes in the FTR context, whereby visual observation of the base confirmed inhomogeneous jet erosion and numerous regions of unperturbed settled beds. This would certainly be a problematic scenario in the HAST operational and POCO context if the physical properties could be inferred to the active HAL solids.

Table II. Sediment Bed Clearance Area Achieved By Each Jet (20s firing in sequence)

Jet	Radius (m)	Peripheral Diameter (m)	Clearance Area (m^2)
Central (continuous)	0.50	-	0.79
Central (in sequence)	0.30	-	0.28
1	0.47	0.94	0.35
2	0.46	1.00	0.36
3	0.50	1.07	0.42
4	0.51	0.92	0.37
5	0.53	0.92	0.38
6	0.52	0.97	0.40

Additionally Regime 4 jet-only erosion profiles were approximately ascertained by measuring the radius and peripheral diameter of the pseudo semi-circular bed clearance patterns (refer to Fig.4(a) expected clearance model and (b) measurements taken). Notably the Central Jet is vertical and creates a circular profile. Upon observation and measurement under the FTR base, all clearance patterns appeared heterogeneous and full clearance was not achieved. Approximate clearance areas obtained via jet-only operation of Regime 4 are summarized in Table II. Akin to the resuspension inhomogeneities established via ABS measurement, the tabulated clearance areas for Jet 1 – 6 illustrate the inhomogeneity of bed erosion by the impinging jets. Ultimately, inhomogeneous and incomplete jet clearance would be problematic from an operational perspective as this would readily impact the formation of radioactive hotspots on the HAST base. Furthermore if there are regions of unperturbed cohesive sediment bed on the base, then this would present significant resuspension challenges from a POCO perspective. Intriguingly the clearance area of the Central Jet is significantly increased where it is fired continuously throughout the cycle in comparison to it being fired in sequence. Therefore perhaps prolonged jet firing enhances bed clearance until maximum clearance is reached, after which point further firing doesn't derive any benefit.

CONCLUSIONS

In summary for all regimes, a relatively simple ABS backscatter profile provided intricate information on sediment bed location, level and success of sediment bed erosion via jet impingement, and visualized sediment resuspension and resettling behavior of jet ballast only and simultaneous airlift operation. Essentially, these data elucidated system dynamics from both a localized and whole system perspective. Additionally, analysis of backscatter profile evolution with time provided information on how the suspension behaves with each operation and how it evolves over time. This feature is particularly useful for the monitoring current plant operation and would enable improved design of future operations (including POCO). Furthermore, a detailed analysis of backscatter profile, i.e. attenuation analysis provided information on

corresponding concentration changes. However in order to verify the concentration changes inferred via empirical attenuation analysis, further work will be conducted in the laboratory on a bench-top scale. Here the attenuation of homogenous Barytes suspensions with varying concentration will be established and the FTR experimental results will be compared with this. Overall the ABS characterization technique has been demonstrated to be powerful tool for the characterization of the distribution of suspended solids within a scaled non-active experimental context. Information obtained via this measurement technique is advantageous for enhancing the understanding of HAST operation, modeling and underpinning POCO operations.

REFERENCES

1 J. BONTHA, K. DENSLOW, H. ADKINS, J. JENKS, C. BURNS, P. SHONEWILL, G. MORGAN, M. GREENWOOD, T. WOOLEY, Evaluation of Three Ultrasonic Instruments for Critical Velocity Determination during Hanford Tank Waste Transfer Operations - 11121. Waste Management Conference. Pheonix Arizona (2011).

2 A. SHUKLA, A. PRAKASH, S. ROHANI, Particles settling studies using ultrasonic techniques, *Powder Technology*, **177**, 2, (2007).

3 R.A. WILLIAMS, C.G. XIE, R. BRAGG, W.P.K. AMARASINGHE, Experimental techniques for monitoring sedimentation in optically opaque suspensions, *Colloids and Surfaces*, **43**, (1990).

4 R.E. CHALLIS, M.J.W. POVEY, M.L. MATHER, A.K. HOLMES, Ultrasound techniques for characterizing colloidal dispersions, *Reports on Progress in Physics*, **68**, 7, (2005).

5 J.R. GRAY and J.W. GARTNER, Technological advances in suspended-sediment surrogate monitoring, *Water Resources Research*, **45**, (2009).

6 S. TEMKIN, Suspension Acoustics: An Introduction of the Physics of Suspensions, Cambridge University Press, (2005).

7 P. HAUPTMANN, N. HOPPE, A. PUTTMER, Application of ultrasonic sensors in the process industry, *Measurement Science & Technology*, **13**, 8, (2002).

8 P.D. THORNE, C.E. VINCENT, P.J. HARDCASTLE, S. REHMAN, N. PEARSON, Measuring suspended sediment concentrations using acoustic backscatter devices, *Marine Geology*, **98**, 1, (1991).

9 M. GUERIN and J.C. SEAMAN, Characterizing clay mineral suspensions using acoustic and electroacoustic spectroscopy, a review, *Clays and Clay Minerals*, **52**, 2, (2004).

10 T.N. HUNTER, L. Darlison, J. Peakall, S. Biggs, Using a multi-frequency acoustic backscatter system as an in situ high concentration dispersion monitor, *Chemical Engineering Science*, 80, (2012).

11 EPM, Mobrey blanket level monitoring [online], Emerson Process Management: Mobrey Measurement Division, <http://www.mobrey.com>, (2009).

12 NIVUS, NivusScope 2 Technical Information [online], NIVUS UK, <http://www.nivus.com>, (2010).

13 G.P. HOLDAWAY, P.D. THORNE, D. FLATT, S.E. JONES, D. PRANDLE, Comparison between ADCP and transmissometer measurements of suspended sediment concentration, *Cont. Shelf Res*., **19**, (1999).

14 R. KOSTASCHUK, J. BEST, P. VILLARD, J. PEAKALL, M. FRANKLIN, Measuring flow velocity and sediment transport with an acoustic Doppler current profiler, *Geomorphology*, **68**, 1-2, (2005).

15 C.P. ROSE and P.D. THORNE, Measurements of suspended sediment transport parameters in a tidal estuary, *Continental Shelf Research*, **21**, 15, (2001).

16 T.N. HUNTER, J. PEAKALL, S. BIGGS, An acoustic backscatter system for in situ concentration profiling of settling flocculated dispersions, *Minerals Engineering*, **27–28**, (2012).

17 S.A. MOORE, G, DRAMAIS, P. DUSSOUILLES, J. LECOZ, C. RENNIE, B. CAMENEN, Acoustic measurements of the spatial distribution of suspended sediment at a site on the Lower Mekong River, ICA Proceedings of Meeting on Acoustics*,* Montreal Canada (2013).

18 N. PAUL, S. BIGGS, M.J. EDMONDSON, T.N. HUNTER, R. HAMMOND, Characterising highly active nuclear waste simulants, *Chemical Engineering Research and Design*, **91**, 4, (2013).

19 G.A. MCARTHUR and J. BUX, Personal communication regarding HAST operation (2013).

20 M.J. QUAYLE, Status of HAL Chemistry Knowledge, Nexia Solutions, Document no: 8327, Issue 1, (2007).

21 G.A. MCARTHUR, T.P. TINSLEY, D. MCKENDRICK, Development of a liquid jet sludge re-suspension model (used on pulse jets or jet ballasts), AIChE Annual Meeting. Cincinnati, OH, USA, pp. 480a/481-480a/414 (2005).

22 T.N. HUNTER and G.A. MCARTHUR, Measuring the erosion and dispersion of sediment beds in impinging-jet ballast tanks, using ultrasonic profilers, IChemE Nuclear fuel cycle conference, Manchester, UK, (2012).

23 J.M. DODDS, Physical Properties of Solid Test Materials for use in Jet-Ballast Experiment Rigs, Current Knowledge February 2012, National Nuclear Laboratory, Document no: HA05950/06/10/06, (2012).

ACKNOWLEDGEMENTS

The authors would like to acknowledge the National Nuclear Laboratory for facility access and Steve Rawlinson for technical support with respect to the rig. Also Sellafield Ltd and George McArthur for general support. And the Nuclear Decommissioning Authority for funding and general support via the National Nuclear Laboratory.